Vibrational spectra of triamantane X18H24, iso-tetramantane X22H28 and cyclohexamantane X26H30 (X = C, Si, Ge, Sn) – A theoretical study

2 **AUTHORS**, INCLUDING:

Ramachandran Gnanasekaran

Academy of Sciences of the Czech Republic

18 PUBLICATIONS **109** CITATIONS

THEO
CHEM

Vibrational spectra of triamantane $X_{18}H_{24}$, *iso*-tetramantane $X_{22}H_{28}$ and cyclohexamantane $X_{26}H_{30}$ (X = C, Si, Ge, Sn) – A theoretical study

Gnanasekaran Ramachandran, Sadasivam Manogaran [*]

Department of Chemistry, Indian Institute of Technology, Kanpur 208016, India

Abstract

Optimized geometrical parameters are obtained for triamantane, *iso*-tetramantane and cyclohexamantane (X = C, Si, Ge, Sn) using B3LYP method with 6-311G** and/or LANL2DZ basis set. For carbon compounds Hartree–Fock (HF) method is also used for the study. The harmonic vibrational frequencies are obtained for all the molecules at their respective optimized geometries. The calculated adamantane frequencies are fitted to the experimental ones of adamantane-d_0 molecule to get the scale factors for C–H stretching frequencies. For all the other modes the scale factors obtained earlier [G. Ramachandran, S. Manogaran, J. Mol. Struct. THEOCHEM, 766 (2006) 125] by fitting all the isotopomers are used. The scale factors thus obtained are used to predict the fundamental frequencies of all carbon compounds and compared to the available experimental Raman frequencies. The assignments are proposed for all fundamentals of the title compounds using normal coordinate analysis.
© 2007 Elsevier B.V. All rights reserved.

Keywords: Triamantane; *iso*-Tetramantane; Cyclohexamantane; Vibrational spectra; Ab initio; DFT calculations

1. Introduction

Adamantane and related structures have interesting electronic properties and applications in chemistry and nanotechnology, because of their highly stable rigid structures. Studies have been carried out on adamantane and the higher diamondoids in order to understand how matter evolves from atoms to bulk as precursors for the synthesis of diamond [2]. In continuation to our earlier work on adamantane (ADA) and diamantane (DIA) [1,3], we present here the results of the study of the higher diamondoid systems, triamantane (TRIA), *iso*-tetramantane (TETRA) and cyclohexamantane (HEXA).

Larger diamondoides [4–9] are created by connecting the adamantane cage to more cages and are categorized according to the number of cages they contain. These hydrocarbons are known to be present in petroleum [10,11]. Till now scientists were able to synthesise up to tetramantane [12] and synthesising higher polymantanes has involved several complications [13]. Depending on the spatial arrangement of adamantane units, higher polymantanes can have numerous isomers and non-isomeric equivalents. Lower adamantologues ADA, DIA and TRIA each have only one isomer. Tetramantane has four isomers, iso-, anti- and two enantiomeric skew forms, respectively. Similarly for hexamantane, there are 39 possible isomers [14]. In the present work we restrict the work to *iso*-tetramantane and cyclohexamantane which is the only diamondoid structure with the formula $C_{26}H_{30}$ [14]. The geometrical parameters of these molecules were studied by molecular mechanics, semi-empirical and ab initio theories by Shen et al. [15]. Experimental Raman spectra of TRIA at different temperatures were reported by Jenkins and Lewis [16]. The report on isolation of HEXA ($C_{26}H_{30}$) crystals by Dahl et al. [14] reawakened the interest in these important class of compounds. The structure of $C_{26}H_{30}$ was determined using X-ray diffraction, mass spectroscopy and $^1H/^{13}C$ NMR spectroscopy [14]. Richardson et al. [17] reanalysed the Raman spectra of HEXA using

DFT method and gave a direct interpretation of the experimental results using the calculated intensities. When we completed our work, the experimental Raman spectra and the theoretical calculations using B3LYP functional with the split valence basis set of Schaefer et al. [18] with polarisation functions on carbon of several diamondoids have been reported by Filik et al. [19]. Their broad selection includes all isomers ranging from adamantane to heptamantane of diamondoid hydrocarbons. It is satisfying to note that the experimental data available from the companion website of this paper [20] agree very well with our predicted frequencies. In this work the authors mentioned, "Differences between the calculated and experimental spectra were found to be most pronounced in CH2/CH bending vibrations, also noticed in our data. The causes of these deficiencies are uncertain but they are most likely due to the use of a relatively small basis set" [19]. Here, we have used a larger basis set and the agreement between the predicted and the experimental fundamentals are very good.

Similar to our earlier paper [1] due to the fundamental importance and potential applications in nanoelectronics, we further extended our studies on these clusters to the other heavier elements of carbon family. For several silicon clusters including ADA, DIA, TRIA, TETRA and adamantane-of-adamantanes (SUPADA), polarizability studies were carried out at HF/6-31++G** level by Mochizuki [21]. The Si-TRIA structure has been studied by MP2/HW-ECP and B3LYP/HW-ECP methods [22]. Apart from this, to the best of our knowledge, no other ab initio or DFT studies on geometry and vibrational frequencies are available.

In this paper, we report the theoretically calculated geometrical parameters and the harmonic frequencies for the three diamondoids TRIA, TETRA and HEXA. Using the scale factors obtained for ADA, the experimental frequencies of the carbon compounds are predicted by scaling their respective force constant matrices. Assignments are made for all the fundamentals based on the normal coordinate calculations. The effects of variations in symmetry and molecular structure on the geometrical parameters and the vibrational frequencies are studied. Spectra are analysed to bring out various similarities and differences among the different diamondoid molecules. We hope that these results will be useful in the further investigation of the heavier diamondoids.

2. Methodology

All computations were carried out using GAUSSIAN 98 and 03 suite of programs [23]. Density functional calculations (DFT) were done using B3LYP functional [24,25] with 6-311G** and/or LANL2DZ basis functions for the X atoms and 6-311++G** for the hydrogens. For carbon compounds additional calculations were done using Hartree–Fock (HF) method using 6-311G** basis set. All molecules are fully optimized and the harmonic frequencies

were obtained at their respective optimized geometries using B3LYP and/or HF methods.

In the evaluation of vibrational force fields, the proper choice of the coordinate system is important [26]. A set of non-redundant $(3N - 6)$ local co-ordinates were constructed as linear combination of the internal coordinates. These local coordinates are used to construct $3N - 6$ symmetry coordinates using the projection operator technique. An orthogonal transformation matrix from the local to the symmetric co-ordinates is obtained using the following equations:

$$U_{ortho} U_{loc} = U_{sym}$$
$$U_{ortho} U_{loc} G_{int} U_{loc}^{\dagger} = U_{sym} G_{int} U_{loc}^{\dagger}$$
$$U_{ortho} G_{loc} = U_{sym} G_{int} U_{loc}^{\dagger}$$
$$U_{ortho} = U_{sym} G_{int} U_{loc}^{\dagger} G_{loc}^{-1}.$$

The cartesian force constants from the Gaussian program [23] are converted to local force constants using the transformation

$$F_{loc} = [(UB)^{-1}]^{\dagger} F_x [(UB)^{-1}]$$

$(UB)^{-1}$ is obtained as follows:

$$(U_{loc} B)^{-1} (U_{loc} B) = E$$
$$(U_{loc} B)^{-1} (U_{loc} B) M^{-1} (U_{loc} B)^{\dagger} = M^{-1} (U_{loc} B)^{\dagger}$$
$$(U_{loc} B)^{-1} G_{loc} = M^{-1} (U_{loc} B)^{\dagger}$$
$$(U_{loc} B)^{-1} = M^{-1} (U_{loc} B)^{\dagger} G_{loc}^{-1}.$$

The ab initio local F is scaled with the scale factors listed in Table 1 and the redundancies in local F are fixed using the procedure described earlier [1]. The local F is then transformed to symmetric F using $U_{ort} F_{loc} U_{ort}^t$ and the eigen value equation $G_{sym} F_{sym} L_{sym} = L_{sym} \Lambda$ is solved [27] to get the Λ and the L_{sym} matrix. The L_{sym} is converted to local L_{loc} by $U_{ort}^t L_{sym}$. The potential energy distributions (PED) are obtained from the diagonal local force constants and the L_{loc} matrix which are used in turn to assign the fundamental frequencies. The C–H stretching scale factors are obtained by fitting the experimental frequencies of ADA-d_0 to the calculated ones using the procedure described in

Table 1
Scale factors for different local coordinates

No.	Local coordinates	Scale factors	
		HF/6-311G**	B3LYP/6-311G**
1	νCC	0.9047	0.9930
2	$\nu C_t H$	0.8364	0.9162
3	$\nu C_s H$	0.8528	0.9337
4	δCH	0.7739	0.9460
5	$\delta_s CH$	0.8383	0.9461
6	δCCC	0.8776	0.9274
7	δCH_2	0.8004	0.9319
8	ωCH_2	0.8070	0.9623
9	τCH_2	0.8252	0.9679
10	ρCH_2	0.8358	0.9640

our earlier papers [3,1]. The other scale factors are obtained by fitting the frequencies of several isotopomers of ADA are taken from our earlier work [1].

3. Geometry

The prime reason for studying these related molecules is to determine their structural similarities and differences and thereby increase our understanding of bonding and structure in general. Each successive higher diamondoid family shows great variation in structural complexity and in the parameters determining their molecular geometries. The optimized geometrical parameters for TRIA,TETRA, HEXA and SUPADA (Figs. 1–4) are given in Tables 2–5. Since the different symmetry makes several equivalent X–X and X–H bonds in each of the molecule, we have several X–X and X–H bond lengths.

In X–H bonds we have two types X_t–H(XH) and X_s–H(XH_2). Although it is experimentally difficult to distinguish these two X–H bonds, since all the theoretical
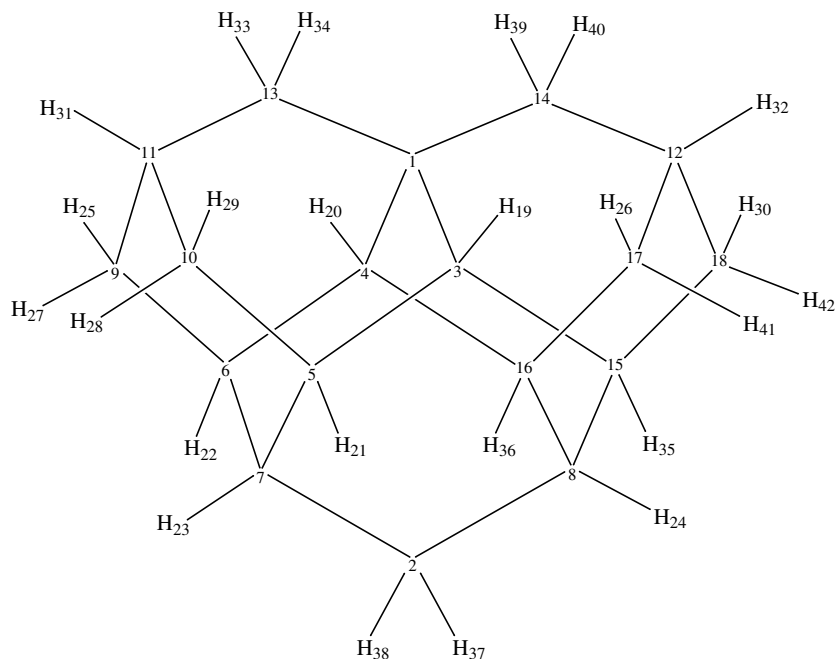

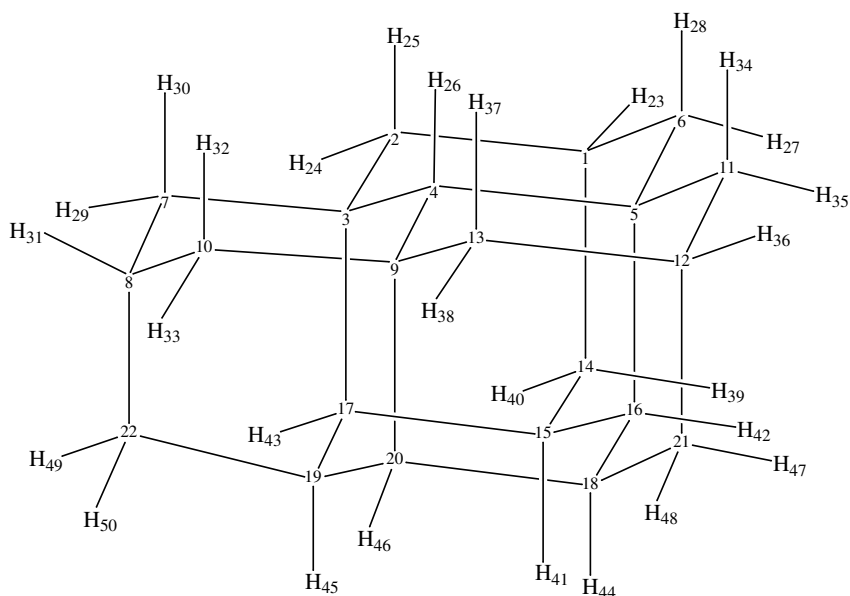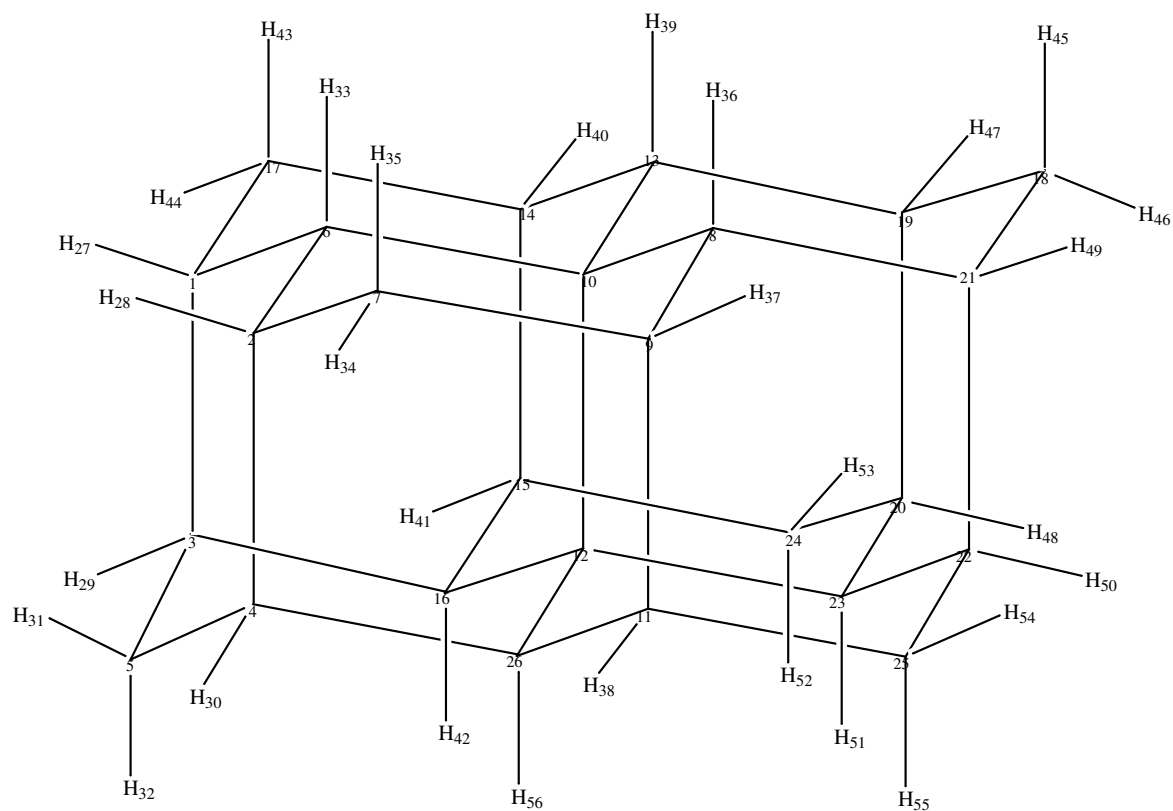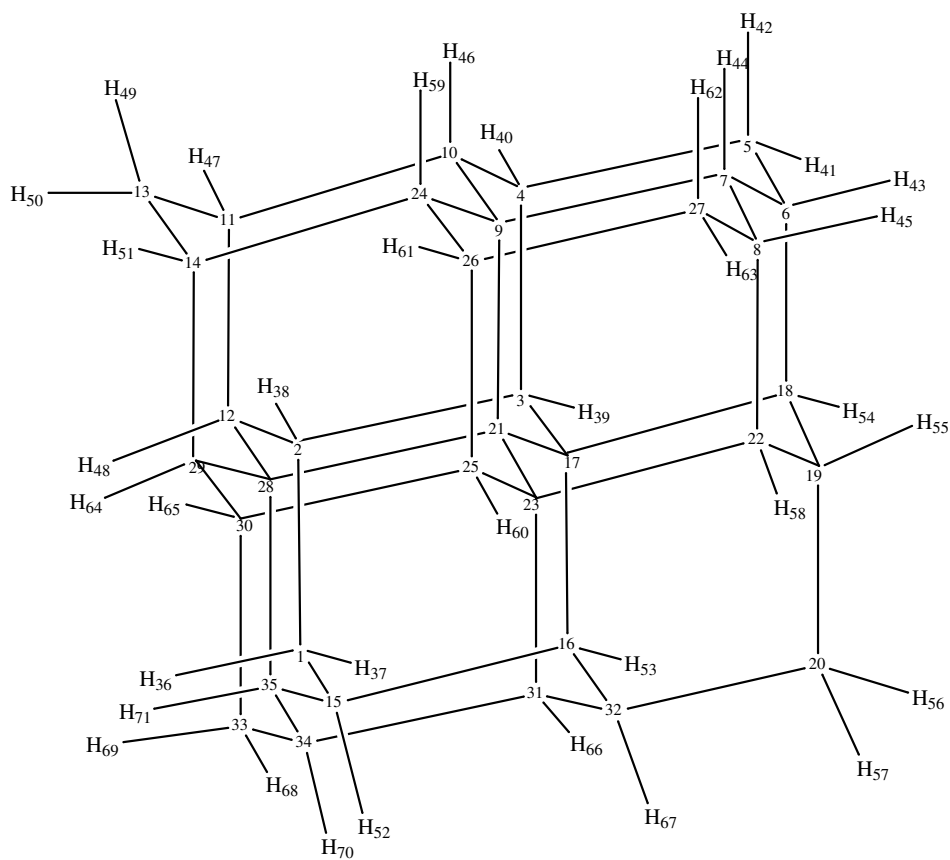Fig. 1. Triamantane ($X_{18}H_{24}$, C_{2v}).

Fig. 2. iso-Tetramantane ($X_{22}H_{28}$, C_{3v}).

Fig. 3. Cyclohexamantane ($X_{26}H_{30}$, D_{3d}).

Fig. 4. Adamantane-of-adamantanes ($X_{35}H_{36}$, T_d).

calculations have established that C–H axial is longer than C–H equatorial in cyclohexane [28], we tried to see whether any consistency exists in all the calculated X–H bond lengths of these related structures. To distinguish C_t–H from C_s–H we calculated these distances in $(CH_3)_3CH$ and $(CH_3)_2CH_2$ by HF, B3LYP and MP2 methods with 6-311G** basis set. The results indicate that C_t–H > C_s–H by 0.001–0.002 Å in all the cases. The experimental values on open shell C_t–H and C_s–H radicals are 1.120 and 1.078 Å [29]. Hence we expect X_t–H > X_s–H which is observed for X = Si, Ge and Sn. In the carbon compounds, this conclu-

sion does not seem to be true and is decided by the nature of the geometrical structure. In ADA and DIA C_s–H > C_t–H. In TRIA and TETRA no definite order exists. In HEXA and SUPADA the C_t–H > C_s–H except for the HF method where they are equal in some cases. TETRA and TRIA show more variation due to lower symmetry.

The experimental bond lengths depend to some extent on the method used to determine them. The electron diffraction values (r_g) are thermally averaged and include anharmonicity and are usually longer than r_e values [30]. X-ray diffraction C–H distances are usually underestimated

Table 2
Bond distances of Triamantane $X_{18}H_{24}$ [distances‡ (Å)]

	$C_{18}H_{24}$			$Si_{18}H_{24}$			$Ge_{18}H_{24}$		$Sn_{18}H_{24}$
	HF A	MP2 A	B3LYP A	HF A	B3LYP A	B3LYP B	B3LYP A	B3LYP B	B3LYP B
X_1X_3 (X_qX_t)	1.551	1.546	1.558	2.383	2.374	2.370	2.481	2.510	2.862
X_1X_{13} (X_qX_s)	1.535	1.532	1.540	2.375	2.368	2.365	2.472	2.504	2.856
X_3X_5 (X_tX_t)	1.540	1.538	1.546	2.377	2.370	2.367	2.474	2.505	2.856
X_5X_7 (X_tX_t)	1.540	1.539	1.547	2.378	2.369	2.365	2.472	2.502	2.852
X_2X_7 (X_tX_s)	1.531	1.532	1.536	2.372	2.364	2.361	2.465	2.497	2.846
X_5X_{10} (X_sX_t)	1.533	1.534	1.538	2.373	2.365	2.362	2.467	2.498	2.848
X_9X_{11} (X_tX_s)	1.534	1.535	1.540	2.373	2.364	2.359	2.463	2.494	2.843
$X_{11}X_{13}$ (X_sX_t)	1.534	1.534	1.539	2.373	2.365	2.361	2.466	2.497	2.846
Dispersion[a]	0.020	0.014	0.022	0.011	0.010	0.011	0.018	0.016	0.019
X_3H_{19} (X_tH)	1.090	1.104	1.099	1.485	1.494	1.479	1.550	1.548	1.718
X_5H_{21} (X_tH)	1.089	1.101	1.098	1.485	1.493	1.478	1.549	1.547	1.717
X_9H_{25} (X_sH)	1.088	1.099	1.097	1.482	1.490	1.476	1.544	1.543	1.712
X_9H_{27} (X_sH)	1.088	1.099	1.096	1.482	1.490	1.476	1.544	1.544	1.712
$X_{11}H_{31}$ (X_tH)	1.088	1.098	1.096	1.484	1.493	1.478	1.548	1.547	1.716
X_7H_{23} (X_tH)	1.089	1.101	1.097	1.485	1.493	1.478	1.549	1.547	1.717
X_2H_{37} (X_sH)	1.089	1.099	1.097	1.482	1.490	1.476	1.544	1.544	1.712
$X_{13}H_{33}$ (X_sH)	1.089	1.101	1.098	1.483	1.491	1.477	1.544	1.544	1.713

A = 6-311G**; B = LANL2DZ ‡ other parameters are available in the supplementary material.
[a] Difference between the longest and the shortest bond lengths.

Table 3
Bond distances of *iso*-tetramantane $X_{22}H_{28}$ [distances‡ (Å)]

	$C_{22}H_{28}$			$Si_{22}H_{28}$			$Ge_{22}H_{28}$		$Sn_{22}H_{28}$
	HF A	MP2 A	B3LYP A	HF A	B3LYP A	B3LYP B	B3LYP A	B3LYP B	B3LYP B
X_3X_4 (X_tX_q)	1.548	1.544	1.556	2.382	2.375	2.373	2.484	2.514	2.867
X_2X_3 (X_qX_s)	1.535	1.532	1.539	2.375	2.368	2.365	2.473	2.505	2.856
X_1X_{14} (X_tX_s)	1.534	1.535	1.539	2.373	2.363	2.358	2.463	2.493	2.841
X_1X_2 (X_tX_s)	1.533	1.534	1.539	2.373	2.365	2.361	2.465	2.496	2.845
X_3X_{17} (X_qX_t)	1.548	1.544	1.555	2.383	2.373	2.369	2.479	2.509	2.860
$X_{14}X_{15}$ (X_tX_s)	1.533	1.533	1.538	2.373	2.365	2.361	2.467	2.498	2.848
$X_{15}X_{16}$ (X_tX_t)	1.537	1.537	1.543	2.377	2.369	2.366	2.473	2.503	2.854
Dispersion[a]	0.015	0.012	0.018	0.009	0.010	0.012	0.019	0.018	0.022
X_4H_{26} (X_tH)	1.092	1.107	1.100	1.486	1.494	1.480	1.551	1.549	1.719
X_2H_{25} (X_sH)	1.089	1.101	1.097	1.483	1.491	1.476	1.544	1.543	1.712
X_2H_{24} (X_sH)	1.089	1.101	1.097	1.483	1.491	1.477	1.544	1.544	1.713
X_1H_{23} (X_tH)	1.088	1.099	1.096	1.485	1.494	1.478	1.548	1.547	1.717
$X_{16}H_{42}$ (X_tH)	1.090	1.104	1.099	1.486	1.494	1.479	1.550	1.548	1.718
$X_{15}H_{41}$ (X_tH)	1.089	1.102	1.098	1.485	1.494	1.478	1.549	1.547	1.717
$X_{14}H_{39}$ (X_sH)	1.088	1.099	1.096	1.482	1.490	1.476	1.544	1.543	1.712

A = 6-311G**; B = LANL2DZ ‡ other parameters are available in the supplementary material.
[a] Difference between the longest and the shortest bond lengths.

Table 4
Bond distances of Cyclohexamantanes $X_{26}H_{30}$ [distances‡ (Å)]

	$C_{26}H_{30}$			$Si_{26}H_{30}$			$Ge_{26}H_{30}$		$Sn_{26}H_{30}$
	HF A	MP2 A	B3LYP A	HF A	B3LYP A	B3LYP B	B3LYP B	B3LYP B	B3LYP B
$X_{12}X_{10}(X_qX_q)$	1.560	1.554	1.569	2.388	2.378	2.374	2.490	2.517	2.871
$X_6X_{10}(X_qX_t)$	1.546	1.542	1.552	2.383	2.375	2.373	2.484	2.515	2.867
$X_1X_6(X_tX_t)$	1.538	1.537	1.545	2.377	2.370	2.367	2.475	2.506	2.857
$X_1X_{17}(X_sX_t)$	1.530	1.531	1.535	2.372	2.364	2.360	2.466	2.497	2.847
$X_1X_3(X_tX_t)$	1.539	1.539	1.545	2.377	2.368	2.363	2.471	2.500	2.850
Dispersion[a]	0.030	0.023	0.034	0.016	0.014	0.014	0.024	0.020	0.024
$X_6H_{33}(X'_tH)$	1.090	1.105	1.099	1.485	1.494	1.479	1.550	1.548	1.718
$X_1H_{27}(X_tH)$	1.089	1.102	1.098	1.485	1.494	1.478	1.549	1.548	1.718
$X_5H_{32}(X'_sH)$	1.089	1.100	1.097	1.482	1.490	1.476	1.544	1.543	1.712
$X_5H_{31}(X_sH)$	1.089	1.100	1.097	1.482	1.491	1.476	1.544	1.544	1.713

A = 6-311G**; B = LANL2DZ ‡ other parameters are available in the supplementary material.

[a] Difference between the longest and the shortest bond lengths.

Table 5
Geometrical Parameters of Adamantane-of-admantanes $X_{35}H_{36}$ [distances‡ (Å)]

	$C_{18}H_{24}$			$Si_{18}H_{24}$			$Ge_{18}H_{24}$	$Sn_{18}H_{24}$
	HF A	MP2 A	B3LYP A	HF A	B3LYP A	B3LYP B	B3LYP B	B3LYP B
$X_{21}X_9(X_qX_q)$	1.556	1.551	1.562	2.388	2.378	2.375	2.519	2.876
$X_9X_{24}(X_qX_t)$	1.544	1.541	1.550	2.382	2.374	2.371	2.513	2.867
$X_{29}X_{14}(X_tX_t)$	1.536	1.536	1.542	2.376	2.369	2.365	2.504	2.855
$X_{13}X_{14}(X_sX_t)$	1.530	1.531	1.535	2.371	2.364	2.360	2.498	2.848
Dispersion[a]	0.026	0.020	0.027	0.017	0.014	0.015	0.021	0.028
$X_{24}H_{59}(X_tH)$	1.091	1.105	1.099	1.486	1.494	1.479	1.549	1.719
$X_{11}H_{47}(X_tH)$	1.089	1.102	1.098	1.485	1.494	1.479	1.548	1.718
$X_{13}H_{49}(X_sH)$	1.089	1.100	1.097	1.483	1.491	1.476	1.544	1.712

A = 6-311G**; B = LANL2DZ ‡ other parameter are available in the supplementary material.

[a] Difference between the longest and the shortest bond lengths.

[15]. For TRIA, TETRA and SUPADA experimental values are not available. For anti-tetramantane, a closely related structure which is not studied here, the values for CH–CH are 1.524 and 1.537 and for C–CH are 1.528 and 1.542 Å, respectively [12]. For HEXA the mean C–C distance is reported as 1.538(7) Å [14]. As expected the

HF distances are less than the B3LYP distances, since HF theory underestimates the bond lengths and inclusion of excited state structures should increase the bond length by inclusion of electron correlation [31]. However the C–C distances obtained from the MP2 method are shorter than the HF values although the C–H distances are in the expected order.

It is noted that the calculated X–X distance varies in a system depending upon the primary/secondary/tertiary/quaternary X connections. The number of different types of unique X–X bonds in each molecule is listed in Table 6. For TRIA and TETRA the bond distances follow the order X–XH > XH–XH > X–XH$_2$ > XH–XH$_2$. The MP2 method predicts shorter C_q–C_s bond compared to other methods. For HEXA and SUPADA the order appears to

Table 6
Number of unique bonds in each system

	TRIA	TETRA	HEXA	SUPADA
$X_q - X_q$	0	0	1	1
$X_q - X_t$	1	2	1	1
$X_q - X_s$	1	1	0	0
$X_t - X_t$	2	1	2	1
$X_t - X_s$	4	3	1	1
$X_s - X_s$	0	0	0	0

Table 7
Distribution of fundamentals among irreducible representations

	Symmetry	Γ_{vib}	Irreducible representations			
			R	IR, R	IR	Inactive
TRIA	C_{2v}	120	$25A_2$	$35A_1 + 29B_1 + 31B_2$		
TETRA	C_{3v}	144		$29A_1 + 48E$		$19A_2$
HEXA	D_{3d}	162	$17A_{1g} + 27E_g$		$16A_{2u} + 27E_u$	$10A_{2g} + 11A_{1u}$

be $X–X > X–XH > XH–XH > XH–XH_2$. The difference between the longest and shortest bond lengths for C–C are 0.022, 0.018, 0.034 and 0.027 Å for TRIA, TETRA, HEXA and SUPADA using B3LYP method. The values for all the methods are listed in the Tables 2–5. The variation is largest for HEXA because it contains $X_q–X_q$ in addition to other types. SUPADA although contains this type bond, because of T_d symmetry the variation is less. TRIA is less symmetric than TETRA which shows up in the variation.

The covalent radii for carbon, silicon, germanium and tin are 0.772, 1.176, 1.223 and 1.405 Å, respectively [32] giving the X–X bond distances as 1.544, 2.352, 2.446 and 2.810 Å, respectively. The values obtained broadly agree with this expectation for several hydrides. The experimentally observed Si–Si values are 2.331, 2.342 Å, respectively,

in Si_2H_6 [33] and Si_6H_{12} [34]. The calculated diamondoid structures are predicted to have longer bonds than these two experimental values. The experimental Si–H bond lengths in some related compounds are Si_2H_6 1.492 [33], Si_6H_{12} 1.484 Å [34]. The values by B3LYP/LANL2DZ method is much shorter than these while B3LYP/6-311G** values are in good agreement. In germanium compounds, the Ge–H distance is similar in 6-311G** and LANL2DZ basis sets. However the Ge–Ge distance differ by 0.03 Å. It is difficult to decide which value is better based on the available experimental values of Ge_2H_6 (2.403) [35], $(Ph_2Ge)_4$ (2.465) [36]. Substituted cyclotrigermane has 2.543 and 2.537 Å as Ge–Ge distance [37]. No experimental data is available for Sn_2H_6 but hexaphenyl-distannane has Sn–Sn distance of 2.79 Å [38]. The Sn–H bond distance in SnH_4 is 1.711 Å [39]. The calculated Sn–H

Table 8
C–H Vibrational frequencies and PED of Adamantane ($C_{10}H_{16}$)

	Expt. [47]	HF				B3LYP				MP2		PED
		6-311G**		aug-cc-pvdz		6-311G**		aug-cc-pvdz		6-311G**		
		Scaled	Unscaled	Scaled	Unscaled	Scaled	Unscaled	Scaled	Unscaled	Scaled	Unscaled	
A_1												
1	2944	2932.8	3187.5	2932.2	3192.4	2925.8	3038.5	2924.4	3045.4	2921.3	3077.1	vC_tH (72), vC_sH (27)
2	2848	2885.1	3142.9	2885.0	3147.8	2885.9	3004.1	2886.0	3011.0	2891.5	3044.9	vC_sH (71), vC_tH (28)
E												
1	2900	2904.3	3145.0	2902.9	3150.3	2906.3	3007.7	2904.0	3013.2	2892.1	3045.0	vC_sH (100)
T_1												
1	–	2931.6	3174.7	2933.4	3150.3	2938.5	3041.1	2941.6	3052.3	2943.6	3099.3	vC_sH (100)
T_2												
1	2944	2942.3	3186.3	2944.0	3195.0	2943.6	3046.4	2946.6	3057.5	2947.9	3103.9	vC_sH (99)
2	2913	2914.1	3170.7	2913.7	3175.9	2912.8	3027.2	2911.6	3035.3	2915.5	3071.5	vC_tH (90)
3	2900	2889.2	3144.1	2889.1	3149.0	2890.1	3006.5	2890.3	3012.4	2892.2	3045.3	vC_sH (90)

Table 9
C–H Vibrational frequencies, and PED of Diamantane ($C_{14}H_{20}$)

	Expt. [16]	HF		B3LYP		MP2		PED
		6-311G**		6-311G**		6-311G**		
		Scaled	Unscaled	Scaled	Unscaled	Scaled	Unscaled	
A_{1g}								
1	2912	2929.7	3186.0	2919.3	3033.7	2917.4	3073.3	vC'_tH (79), vC_sH (17)
2	2885	2894.4	3164.8	2890.2	3017.3	2899.3	3054.0	vC_tH (52), vC_sH (32), vC'_tH (16)
3	2848	2884.0	3140.0	2878.4	2996.7	2883.5	3036.9	vC_sH (50), vC_tH (45)
A_{2g}								
1	–	2931.4	3174.3	2931.1	3033.6	2940.5	3096.0	vC_sH (100)
E_g								
1	–	2939.1	3183.1	2936.5	3039.3	2943.5	3099.2	vC_sH (99)
2	2897	2907.2	3150.8	2901.5	3004.3	2891.1	3044.1	vC_sH (90)
3	2872	2873.4	3139.1	2867.9	2994.5	2879.0	3033.3	vC_tH (89)
A_{1u}								
1	–	2931.2	3174.1	2930.9	3033.3	2940.3	3095.8	vC_sH (100)
A_{2u}								
1	–	2921.3	3176.6	2913.1	3028.6	2915.7	3071.7	vC'_tH (87), vC_sH (12)
2	–	2889.5	3147.1	2888.1	3003.8	2890.8	3043.9	vC_sH (81), vC'_tH (13)
3	–	2871.5	3139.0	2865.8	2993.5	2876.5	3030.7	vC_tH (93)
E_u								
1	–	2940.2	3184.5	2937.5	3040.4	2944.2	3099.9	vC_sH (99)
2	–	2910.6	3161.2	2903.8	3011.9	2895.0	3048.8	vC_sH (63), vC_tH (37)
3	–	2880.3	3139.7	2873.7	2995.5	2882.0	3035.7	vC_tH (63), vC_sH (37)

bond lengths agree well with this value. The bond angles deviate from the ideal tetrahedral value. The XXH angles are close to 109.6° and the HCH angle is more closer to 107° in carbon compounds and 108° in the heavier analogues. Similar results were obtained for cyclohexane and sila-cyclohexane [28]. Since the data available for the heavier analogues are only for small molecules, it is difficult to assess the accuracy of the calculated geometrical parameters and their variation for these heavier analogues since the nature of bonding varies as we go from C to Sn. However the present data will give an idea about the relative values.

4. Vibrational spectra

The non-redundant local coordinates are chosen to be similar to that of ADA so that the scale factors of ADA could be transferred to TRIA, TETRA and HEXA molecules. It is not clear whether the scale factors of ADA are suitable for the heavier analogues. Urban et al. [40] used the scale factors of C_2H_6 to the predict the frequencies of Si_2H_6 and Ge_2H_6. Since LANL2DZ is designed for heavier

elements it is also not clear how the scale factors will differ from that of 6-311G**. We tried to get the scale factors for B3LYP method using LANL2DZ and 6-311G** basis sets for Si_2H_6 and Ge_2H_6. However the scale factors are not consistent. Hence we have not scaled the frequencies for non-carbon compounds. More experimental data is needed to arrive at good scale factors for these compounds.

The molecules studied in the present work, TRIA, TETRA and HEXA are all saturated hydrocarbons with sp^3 carbon atoms having a rigid structure. It is not surprising that the CC, CH and CH_2 stretchings and HCH, HCC and CCC bendings appear in the regions where they are usually expected. HEXA (D_{3d}) being more symmetric has 118 lines while the less symmetric TETRA (C_{3v}) has 96 and TRIA (C_{2v}) has 120. The more compact structures of these molecules undoubtedly exhibit the structural differences in the ranges of characteristic frequencies observed in their vibrational spectra. The carbon frame work is the rigid part and hence the vibrations associated with carbon skeleton should reflect the rigidity as we move to higher diamondoids. The diamond is rigid because all carbons are quaternary. When quaternary carbons are involved in

Table 10
C–H Vibrational frequencies and PED of Triamantane ($C_{18}H_{24}$)

No.	Expt. [20]	Scaled		Unscaled				PED
		B3LYP	HF	B3LYP	I		HF	
					R	IR		
A_1								
1	–	2939.4	2938.6	3042.2	207.6	99.7	3182.9	νC_9H_{27} (54), νC_9H_{25} (45)
2	2918	2917.8	2925.7	3031.7	1043.1	9.9	3181.0	νC_9H_{25} (33), νC_9H_{27} (28) $\nu C_{11}H_{31}$ (14), $\nu C_{13}H_{33}$ (10)
3	2910	2906.2	2912.2	3019.8	221.6	184.5	3166.6	νC_2H_{37} (81)
4	2896	2899.2	2904.1	3006.8	84.9	10.7	3150.0	$\nu C_{13}H_{33}$ (71), νC_9H_{25} (13)
5	2892	2887.7	2888.7	3000.2	92.6	53.2	3145.1	$\nu C_{11}H_{31}$ (72), $\nu C_{13}H_{33}$ (11)
6	2880	2878.9	2882.1	2997.7	43.8	44.9	3139.6	νC_5H_{21} (50), νC_7H_{23} (21)
7	2864	2869.6	2872.6	2994.5	61.7	5.1	3135.4	νC_7H_{23} (67), νC_5H_{21} (26)
8	2850/2840	2856.8	2862.4	2983.9	4.2	23.0	3128.4	νC_3H_{19} (87), νC_5H_{21} (11)
A_2								
1	–	2935.5	2933.6	3038.0	0.9	–	3176.7	νC_9H_{25} (51), νC_9H_{27} (45)
2	2925	2924.6	2924.4	3026.7	2.9	–	3166.8	$\nu C_{13}H_{33}$ (96)
3	2910	2904.6	2906.7	3008.2	65.0	–	3151.5	νC_9H_{27} (51), νC_9H_{25} (46)
4	2864	2867.9	2870.7	2994.0	2.6	–	3135.0	νC_5H_{21} (96)
B_1								
1	–	2937.2	2938.7	3039.9	148.1	128.1	3182.9	νC_9H_{25} (43), νC_9H_{27} (36) $\nu C_{13}H_{33}$ (19)
2	–	2932.9	2934.1	3035.6	140.8	44.8	3178.1	νC_2H_{37} (98)
3	2925	2929.6	2929.2	3031.9	9.4	252.2	3172.0	$\nu C_{13}H_{33}$ (80), νC_9H_{27} (11)
4	2910	2905.4	2908.1	3011.8	9.4	252.2	3157.7	νC_9H_{27} (50), νC_9H_{25} (45)
5	2880	2875.1	2880.1	2998.6	102.2	4.3	3139.7	νC_5H_{21} (88)
6	2840/2850	2855.3	2860.3	2982.9	61.0	13.3	3127.2	νC_3H_{19} (92)
B_2								
1	–	2938.8	2937.7	3041.5	110.6	60.9	3181.5	νC_9H_{27} (54), νC_9H_{25} (46)
2	2910	2913.9	2919.5	3028.2	51.2	212.4	3173.9	νC_9H_{25} (40), νC_9H_{27} (34) $\nu C_{11}H_{31}$ (17)
3	2896	2895.6	2899.1	3011.6	157.9	46.2	3156.2	$\nu C_{13}H_{33}$ (63), $\nu C_{11}H_{31}$ (18)
4	2892	2886.1	2886.2	3001.6	0.7	1.9	3142.1	$\nu C_{11}H_{31}$ (60), $\nu C_{13}H_{33}$ (29)
5	2880	2877.5	2880.9	2993.3	0.9	9.6	3135.9	νC_7H_{23} (68), νC_5H_{21} (26)
6	2864	2865.9	2868.2	2993.0	26.7	27.6	3134.5	νC_5H_{21} (68), νC_7H_{23} (29)

I-Intensities (B3LYP, IR: km mole^{-1} R: Å^{4}amu^{-1}).

the stretching and bending, the force constants are expected to be higher. The C–H next to a quaternary carbon has the lowest frequency.

The CH stretching region, 2800–3000 cm^{-1}, is usually complicated by severe overlap of different modes and the line shapes are usually broad. In addition to the stretching fundamentals, overtones and combinations can occur between the fundamentals and Fermi resonances can occur. Also the harmonic approximation usually assumed is not strictly valid in this region because of considerable anharmonicity in the CH stretchings. As a result the assignment becomes very difficult. Since the assignments of CH stretching region of ADA and DIA in our earlier work [1] is not satisfactory, we have included the revised assignments for the νCH region for ADA and DIA also. We fitted the frequencies of only ADA-d_0 to the experimental values.(In the earlier we fitted several isotopomer frequencies). The scale factors obtained by fitting the calculated frequencies to the experimental ones of ADA-d_0 are used to predict the CH frequencies of DIA,TRIA, TETRA and HEXA. For the prediction of other fundamentals we used the same scale factors of our earlier paper [1]. The agreement is excellent with the experimental Raman frequencies. The X–H bond lengths for X = Si, Ge and Sn clearly has two distinct regions giving X–H > X–H$_2$. Hence a similar trend of νX–H appearing

at lower frequencies compared to νX–H$_2$ appears to be true. However in X = C, this kind of clear distinction does not follow.

The δCH$_2$ modes are more or less pure modes. The linear combinations of CH$_2$ groups leads to different irreducible representations. The number of methylene groups in the three systems are 7, 9 and 6, respectively. The different extent of mixing the CH$_2$s give the range of frequencies. Because of the symmetry the CH$_2$s in HEXA are similar compared to TRIA and TETRA. The variation is larger for TRIA and TETRA and HEXA has a smaller variation. The symmetry labels and the scaled frequencies in cm^{-1} for B3LYP/6-311G** are as follows: TRIA-A_1: 1458, 1447, 1441; A_2 1437; B_1: 1436; B_2: 1455, 1435; TETRA-A_1 1453, 1435; A_2: 1428; E 1450,1437,1431; HEXA-A_{1g}: 1441; A_{2u}: 1443; E_g: 1443; E_u: 1442. These frequencies are very close to those of cyclohexane [28], ADA and DIA [1] confirming that the force fields for these structurally related molecules are very similar.

The symmetry, number of discrete vibrational frequencies (Γ), IR, Raman active and inactive modes for all the systems were listed in Table 7. Along with the available experimental frequencies the scaled and unscaled HF and B3LYP frequencies for C–H stretching using 6-311G** and/or LANL2DZ basis set are listed in Tables 8–12.

Table 11
C–H Vibrational frequencies and PED of *iso*-tetramantane (C$_{22}$H$_{28}$)

No.	Expt. [20]	Scaled		Unscaled				PED
		B3LYP	HF	B3LYP	I		HF	
					R	IR		
*A*1								
1	–	2933.3	2938.8	3036.1	279.9	185.2	3183.0	νC$_2$H$_{25}$ (53), νC$_2$H$_{24}$ (45)
2	2914	2915.0	2924.2	3029.3	1134.6	3.4	3179.1	νC$_{14}$H$_{39}$ (45), νC$_2$H$_{25}$ (17) νC$_1$H$_{23}$ (17), νC$_2$H$_{24}$ (14)
3	2902	2900.4	2906.7	3013.3	260.2	207.5	3162.9	νC$_{14}$H$_{39}$ (45), νC$_2$H$_{24}$ (30) νC$_2$H$_{25}$ (18)
4	2894	2886.1	2889.8	2999.9	132.8	89.1	3146.0	νC$_1$H$_{23}$ (74)
5	2871	2877.4	2884.0	2998.2	88.6	30.0	3141.0	νC$_{15}$H$_{41}$ (75)
6	2862	2853.9	2863.4	2980.8	46.6	0.0	3129.6	νC$_{16}$H$_{42}$ (83), νC$_{15}$H$_{41}$ (13)
7	2848	2839.4	2851.9	2965.9	9.6	18.4	3117.2	νC$_4$H$_{26}$ (96)
*A*2								
1	–	2935.5	2935.2	3038.1	–	–	3178.5	νC$_{14}$H$_{39}$ (96)
2	–	2921.8	2922.4	3023.9	–	–	3164.6	νC$_2$H$_{25}$ (49), νC$_2$H$_{24}$ (48)
3	–	2889.9	2895.5	2990.7	–	–	3135.4	νC$_2$H$_{24}$ (50), νC$_2$H$_{25}$ (50)
E								
1	–	2937.0	2938.4	3039.8	211.2	108.6	3182.4	νC$_{14}$H$_{39}$ (88)
2	–	2928.5	2931.5	3030.9	23.3	13.7	3174.5	νC$_2$H$_{25}$ (49), νC$_2$H$_{24}$ (43)
3	2924	2923.7	2925.2	3025.9	7.2	42.6	3172.3	νC$_2$H$_{25}$ (50), νC$_2$H$_{24}$ (46)
4	2914	2910.2	2917.4	3025.8	88.8	154.8	3167.6	νC$_{14}$H$_{39}$ (60), νC$_1$H$_{23}$ (19), νC$_2$H$_{25}$ (11)
5	2902	2898.0	2904.0	3006.7	92.4	24.3	3152.0	νC$_2$H$_{24}$ (33), νC$_{14}$H$_{39}$ (31) νC$_2$H$_{25}$ (25)
6	2894	2893.8	2899.9	2997.4	86.3	70.6	3144.1	νC$_2$H$_{25}$ (44), νC$_2$H$_{24}$ (42)
7	–	2884.0	2884.8	2992.4	1.4	0.5	3136.0	νC$_1$H$_{23}$ (63), νC$_2$H$_{24}$ (18) νC$_2$H$_{25}$ (16)
8	2871	2866.7	2873.1	2991.6	0.3	10.4	3135.8	νC$_{15}$H$_{41}$ (87)
9	2862	2852.6	2861.7	2979.7	26.1	25.7	3128.2	νC$_{16}$H$_{42}$ (89)

I-Intensities (B3LYP, IR: km mole^{-1} R: Å^{4}amu^{-1}).

Table 12
C–H Vibrational frequencies and PED of Cyclohexamantane ($C_{26}H_{30}$)

No.	Expt. [20]	Scaled		Unscaled				PED
		B3LYP	HF	B3LYP	I		HF	
					R	IR		
A_{1g}								
1	–	2932.0	2933.8	3034.9	434.5	–	3179.4	vC_5H_{32} (51), vC_5H_{31} (48)
2	2912	2911.1	2921.0	3024.8	1592.0	–	3177.0	vC_5H_{31} (38), vC_5H_{32} (38)
								vC_1H_{27} (20)
3	2878	2876.9	2882.8	2993.4	38.9	–	3137.1	vC_1H_{27} (68), vC_5H_{31} (14)
4	2860	2858.0	2867.9	2985.6	211.5	–	3134.5	vC_6H_{33} (87), vC_1H_{27} (11)
A_{2g}								
1	–	2864.0	2867.1	2992.1	–	–	3135.1	vC_1H_{27} (99)
E_g								
1	–	2931.8	2933.1	3034.4	139.8	–	3176.7	vC_5H_{32} (51), vC_5H_{31} (49)
2	2901	2902.9	2909.0	3009.0	158.4	–	3156.6	vC_5H_{31} (48), vC_5H_{32} (46)
3	2878	2876.0	2883.0	3003.5	231.1	–	3150.6	vC_1H_{27} (94)
4	2860	2867.2	2871.0	2991.7	75.7	–	3134.1	vC_1H_{27} (94)
5	2848	2847.7	2856.8	2975.0	8.3	–	3123.6	vC_6H_{33} (94)
A_{1u}								
1	–	2872.7	2877.9	3001.2	–	–	3146.9	vC_1H_{27} (99)
A_{2u}								
1	–	2933.0	2934.8	3035.9	–	213.5	3179.2	vC_5H_{32} (51), vC_5H_{31} (48)
2	–	2902.9	2909.1	3008.7	–	275.1	3157.0	vC_5H_{31} (51), vC_5H_{32} (44)
3	–	2871.1	2877.5	2995.1	–	0.5	3138.8	vC_1H_{27} (87)
4	–	2855.5	2866.6	2982.9	–	132.4	3134.1	vC_6H_{33} (90)
E_u								
1	–	2931.6	2933.0	3034.2	–	69.6	3176.7	vC_5H_{32} (51), vC_5H_{31} (48)
2	–	2906.0	2913.8	3016.7	–	394.1	3167.4	vC_5H_{31} (43), vC_5H_{32} (43)
								vC_1H_{27} (13)
3	–	2876.1	2882.5	2998.5	–	30.4	3143.4	vC_1H_{27} (84)
4	–	2865.0	2868.2	2990.1	–	20.8	3132.0	vC_1H_{27} (96)
5	–	2848.4	2857.2	2975.7	–	9.6	3124.1	vC_6H_{33} (94)

I-Intensities (B3LYP, IR: km mole^{-1} R: Å^{4}amu^{-1}).

The other frequencies are available in the supplementary material. It is clear from the tables that both HF and B3LYP results match well with the experimental values. The RMS deviations for TRIA, TETRA and HEXA for 88, 62 and 37 experimental frequencies, respectively, are 7.2, 6.1, 7.3 cm^{-1} for B3LYP/6-311G** and 9.5, 13.5, 14.8 cm^{-1} for HF/6-311G**. We have also given the calculated intensities for the carbon compounds in the Tables. The agreement with the experimental values is not very satisfactory.

In the heavier molecules, the X–H and X–X bonds become weaker as we go from X = C to Sn. This is reflected in their frequencies. The Si–H experimental frequencies in the smaller molecules are Si_2H_6: 2163, 2154, 2179, 2155 cm^{-1} [41]. SiH_4: 2185.7, 2189.1 cm^{-1} [42]. The matrix isolation IR spectra of Si_3H_8 and Si_4H_{10} are available in the literature [43]. The calculated frequencies for vSi–H appear in the range 2162–2201 cm^{-1} for B3LYP/6-311G** method and 2183–2217 cm^{-1} for B3LYP/LANL2DZ. The calculated frequencies are in agreement with the above experimental values for the B3LYP/6-311G** method. Using LANL2DZ basis set yields higher numbers. For Ge–H, the experimental values are Ge_2H_6: 2068, 2077.1, 2090.7 cm^{-1} [44]. GeH_4: 2110, 2111 cm^{-1} [45]. The calculated range 2045–2095 cm^{-1} is in agreement with these values. The Sn–H in Sn_2H_6 occur at 1840 cm^{-1} in the experiment [46]. The range of calculated numbers are 1846–1894 cm^{-1}. It appears that the calculated frequencies for the heavier analogues are very close to the experimental values and the scale factor will be very close to 1.0 for these molecules. All the assignments are given in Tables S 13-17. The assignments are straight forward from the tables and hence are not discussed further.

5. Conclusions

Symmetry dictates the variations in the bond lengths to a large extent, although the nature of bonding also plays a role in determining the final values. The geometrical parameters obtained from the optimized structures indicate X_t–H (XH) is greater than X_s–H (XH_2) for X = Si, Ge and Sn. The predicted frequencies using the scale factors of ADA obtained by the SQM procedure agree very well with the experimental Raman frequencies for the carbon compounds. For the non-carbon compounds the calculated frequencies are closer to the experimental frequencies of small molecules indicating a scale factor closer to 1. Probable assignments are made for all the fundamentals of the title compounds.

Acknowledgement

This study is supported in part by a Grant from the Department of Science and Technology, New Delhi.

Appendix A. Supplementary data

Internal and local coordinates, geometrical parameters, the assignments of the vibrational frequencies for TRIA, TETRA and HEXA are given as supplementary material (Figures S1–S3 and Tables S1–S12).

Supplementary data associated with this article can be found, in the online version, at doi:10.1016/j.theochem.2007.03.038.

References

[1] G. Ramachandran, S. Manogaran, J. Mol. Struct. THEOCHEM 766 (2006) 125.
[2] A.K. Sharma, J. Narayan, Int. Mater. Rev. 4 (1997) 137.
[3] D. Ragubanshi, S. Maheshwary, S. Manogaran, J. Mol. Struct. THEOCHEM 574 (2001) 245.
[4] C.A. Cupas, P.v.R. Schleyer, D.J. Trecker, J. Am. Chem. Soc. 87 (1965) 917.
[5] V.Z. Williams Jr., P.v.R. Schleyer, G.J. Gleicher, L.B. Rodewald, J. Am. Chem. Soc. 88 (1966) 3862.
[6] D. Farcasiu, H. Bohm, P.v.R. Schleyer, J. Org. Chem. 42 (1977) 96.
[7] G.A. Mansoori, J. Pet. Sci. Eng. 17 (1997) 101.
[8] D. Vazquez Gurrola, J. Escobedo, G.A. Mansoori, Characterization of Crude Oils from Southern Mexican Oil Fields, in: EXITEP, 1998, Proceedings, Mexico City, Mexico.
[9] J.E. Dahl, S.G. Liu, R.M.K. Carlson, Science 299 (2003) 96.
[10] R. Lin, Z.A. Wilk, Fuel 74 (1995) 1512.
[11] J.E. Dahl, J.M. Moldowan, K.E. Peters, G.E. Claypool, M.A. Rooney, G.E. Michael, M.R. Mello, M.L. Kohnen, Nature 399 (1999) 54.
[12] W. Burns, M.A. McKervey, T.R.B. Mitchell, J.J. Rooney, J. Am. Chem. Soc. 100 (1978) 906.
[13] E. Ozawa, A. Furusaki, N. Hashiba, T. Matsumoto, V. Sing, Y. Tahara, E. Wiskott, M. Farcasiu, T. Iizuka, N. Tanaka, T. Kan, P.v.R. Schleyer, J. Org. Chem. 45 (1980) 2985.
[14] J.E.P. Dahl, J.M. Moldowan, T.M. Peakman, J.C. Cardy, E. Lobkovsky, M.M. Olmstead, P.W. May, T.J. Davis, J.W. Steeds, K.E. Peters, A. Pepper, A. Ekuan, R.M.K. Carlson, Angew. Chem., Int. 42 (2003) 2040.
[15] M. Shen, H.F. Schaefer III, C. Liang, J.-H. Lii, N.L. Allinger, P.v.R. Schleyer, J. Am. Chem. Soc., 192, 114, 497.
[16] T.E. Jenkins, J. Lewis, Spectrochim. Acta 36A (1979) 259.
[17] S.L. Richardson, T. Baruah, M.J. Mehl, M.R. Pederson, Chem. Phys. Lett. 403 (2005) 83.
[18] A. Schaefer, H. Horn, R. Ahlrichs, J. Chem. Phys. 97 (1992) 2571.
[19] J. Filik, J.N. Harvey, N.L. Allan, P.W. May, J.E.P. Dahl, S. Liu, R.M.K. Carlson, Spectrochim. Acta 64A (2005) 681.
[20] www.chm.bris.ac.uk/pt/diamond/diamondoids.htm.
[21] Y. Mochizuki, H. Agren, Chem. Phys. Lett. 336 (2001) 451.
[22] Y. Ge, J.D. Head, J. Phys. Chem. 106B (2002) 6997.
[23] M.J. Frisch et al., Gaussian 03 Revision C.02, Gaussian, Inc., Wallingford, CT, 2004.
[24] A.D. Becke, J. Chem. Phys. 98 (1993) 5648.
[25] C. Lee, W. Yang, R.G. Parr, Phys. Rev. 37B (1988) 785.
[26] P. Pulay, G. Fogarasi, F. Pang, J.E. Boggs, J. Am. Chem. Soc. 101 (1979) 2550.
[27] E.B. Wilson, J.C. Decius, P.C. Cross, Molecular Vibrations, McGraw-Hill, New York, 1955.
[28] M.K. Leong, V.S. Mastryukov, J.E. Boggs, J. Phys. Chem. 98 (1994) 6961.
[29] W.J. Hehre, L. Radom, P.v.R. Schleyer, J.A. Pople, Ab Initio Molecular Orbital Theory, John Wiley, New York, 1986.
[30] M. Hargittai, I. Hargittai, Int. J. Quantum Chem. 44 (1992) 1057.
[31] C.J. Cramer, Essentials of Computational Chemistry, John Wiley, New York, 2002.
[32] N.N. Greenwood, A. Earnshaw, Chemistry of the Elements, Pergamon Press, Oxford, 1984.
[33] B. Beagley, A.R. Conrad, J.M. Freeman, J.J. Monaghan, B.G. Norton, G. Holywell, J. Mol. Struct. 11 (1972) 371.
[34] Z. Smith, A. Almenningen, E. Hengge, D. Kovar, J. Am. Chem. Soc. 104 (1982) 4362.
[35] B. Beagley, J.J. Monaghan, Trans. Faraday Soc. 66 (1970) 2745.
[36] L. Ross, M. Drager, J. Organomet. Chem. 199 (1980) 195.
[37] S. Masamune, Y. Hanzawa, D.J. Williams, J. Am. Chem. Soc. 104 (1982) 6136.
[38] H. Preut, H.J. Haupt, F.Z. Huber, Z. Anorg. Allg. Chem. 396 (1973) 81.
[39] H.W. Kattenberg, A. Oskam, J. Mol. Spectrosc. 51 (1974) 377.
[40] J. Urban, P.R. Schreiner, G. Vacek, P.v.R. Schleyer, J.Q. Huang, J. Leszczynski, Chem. Phys. Lett. 264 (1997) 441.
[41] J.R. Durig, J.S. Church, J. Chem. Phys. 73 (1980) 4784.
[42] H.W. Kattenberg, A. Oskam, J. Mol. Spectrosc. 49 (1974) 52.
[43] B. Albinsson, H. Teramae, H.S. Plitt, L.M. Goss, H. Schmidbaur, J. Michl, J. Phys. Chem. 100 (1996) 8681.
[44] J.E. Griffiths, G.E. Walrafen, J. Chem. Phys. 40 (1964) 321.
[45] H.W. Kattenberg, W. Gabes, A. Oskam, J. Mol. Spectrosc. 44 (1972) 425.
[46] W.L. Jolly, Angew. Chem. 72 (1960) 268;
J. Chem. Soc. 83 (1961) 335.
[47] L. Bistricic, G. Baranovic, K.M. Majerski, Spectrochim. Acta 51A (1995) 1643.